Supplement of The Cryosphere, 19, 2507–2526, 2025
https://doi.org/10.5194/tc-19-2507-2025-supplement

The Cryosphere Open Access EGU

Supplement of

Aspect controls on the spatial redistribution of snow water equivalence through the lateral flow of liquid water in a subalpine catchment

Kori L. Mooney and Ryan W. Webb

Correspondence to: Ryan W. Webb (ryan.webb@uwyo.edu)

Snow Temperature Observations in order of collection date.

Table S1. Flat aspect snow pit observed temperatures for 12 Jan.

Height above Ground (cm)	Temperature (°C)
172	-5.0
152	-3.0
132	-3.0
112	-2.0
92	-2.0
72	-1.0
52	-1.0
32	0.0
12	0.0

Table S2. Base of south aspect snow pit observed temperatures for 6 Feb.

Height above Ground (cm)	Temperature (°C)
90	-2.5
10	0.0

Table S3. Base of south aspect snow pit observed temperatures for 28 Feb.

Height above Ground (cm)	Temperature (°C)
175	-1.0
125	-2.0
75	-1.0
30	0.0

Table S4. Flat aspect snow pit observed temperatures for 1 Apr.

Height above Ground (cm)	Temperature (°C)
241	0.0
231	-2.0

221	-2.0
201	-1.5
193	-1.5
178	-1.0
168	-1.0
155	-1.0
145	-1.0
133	-1.0
123	-1.0
113	-1.0
100	-1.0
90	-0.5
80	-0.5
70	0.0
60	0.0
50	0.0
40	0.0
30	0.0
17	0.0
10	0.0

Table S5. North aspect snow pit observed temperatures for 1 Apr.

Height above Ground (cm)	Temperature (°C)
235	0.0
225	-2.0
215	-2.0
205	-2.5
295	-2.0
185	-1.0
175	-1.0
165	-1.0
155	-1.0
145	-1.0
135	-1.0

125	-1.0
115	-1.0
105	-1.0
95	-1.0
85	-1.0
75	-1.0
65	-1.0
55	-1.0
45	-1.0
35	-1.0
25	-1.0
15	-1.0
5	0.0

Table S6. Base of south aspect snow pit observed temperatures for 1 Apr.

Height above Ground (cm)	Temperature (°C)
222	-0.5
172	0.0
122	0.0
72	0.0
22	0.0

Table S7. Base of south aspect snow pit observed temperatures for 1 May.

Height above Ground (cm)	Temperature (°C)
125	0.0
100	0.0
75	0.0
50	0.0
25	0.0
0	0.0

The following Images are minimally processed radargrams. Note that while there is some time-zero correction, the processing for the project used ReflexW semi-automatic picking for both the snow surface (time zero) and subtract that from the reflection of the snow-soil interface. In the below images, the x-axis is the trace number of the raw ground penetrating radar measurement, and the y-axis is the two-way traveltime of the reflection (ns). The captions of the figures indicate the date, aspect, and location on hillslope.

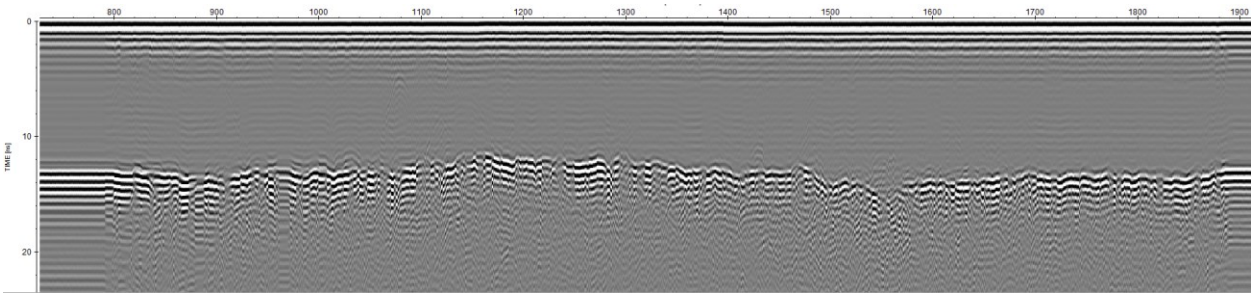

Figure S1. 12 Jan Flat aspect radargram.

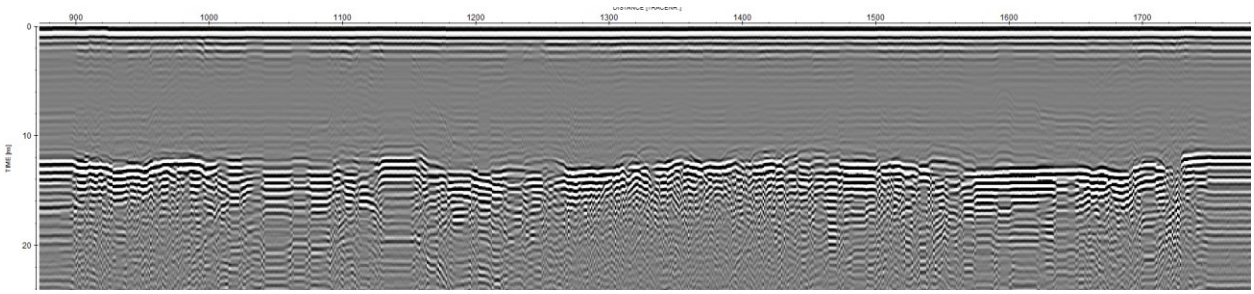

Figure S2. 12 Jan South Base radargram.

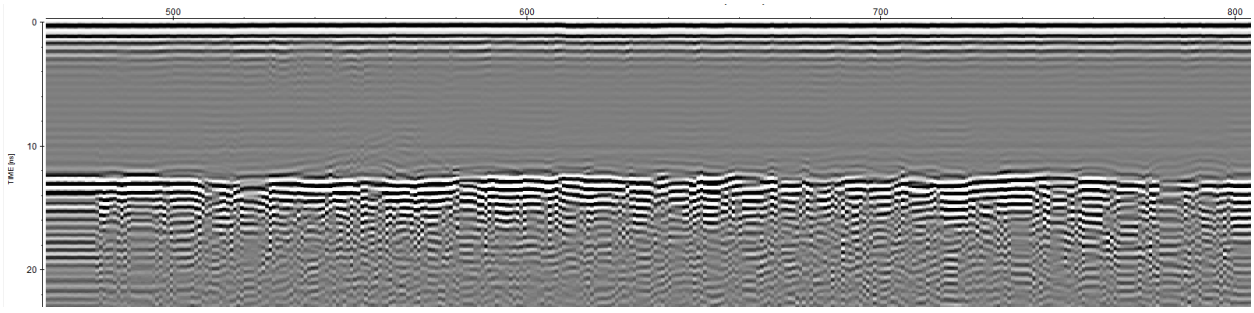

Figure S3. 12 Jan South Middle radargram.

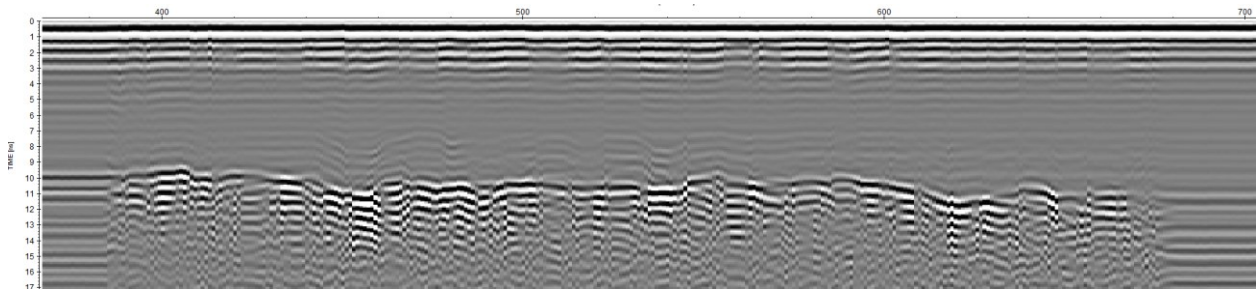

Figure S4. 12 Jan South Top radargram.

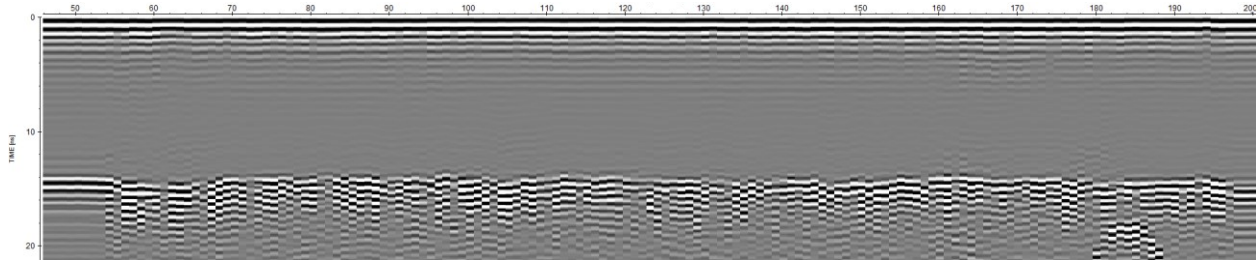

Figure S5. 6 Feb Flat aspect radargram.

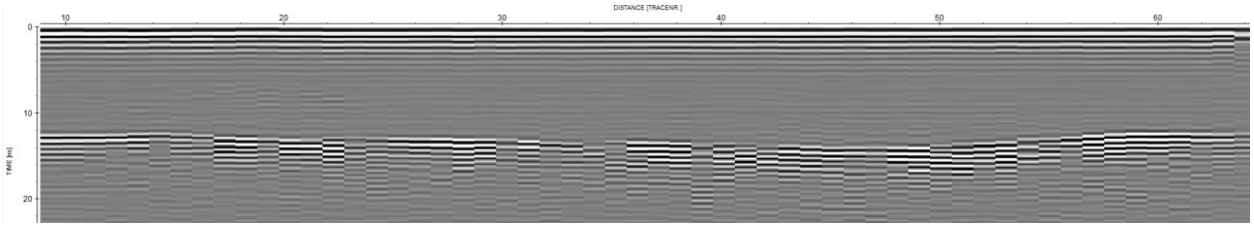

Figure S6. 6 Feb North Base radargram.

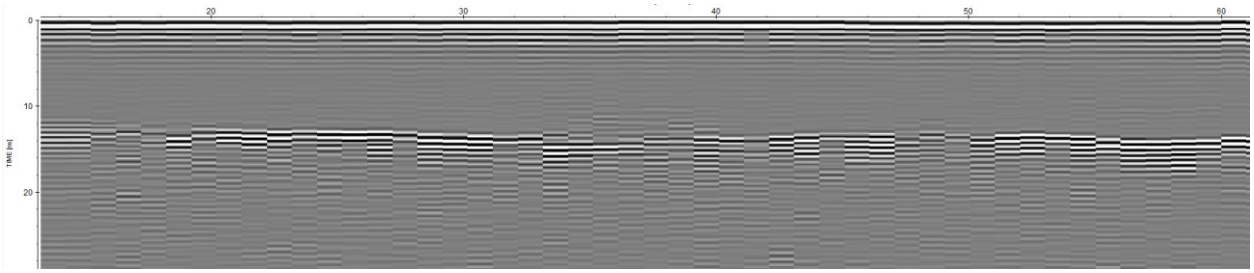

Figure S7. 6 Feb North Middle radargram.

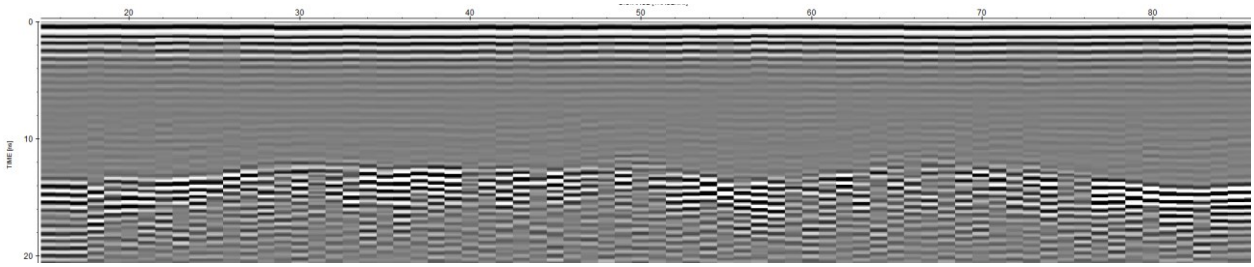

Figure S8. 6 Feb North Top radargram.

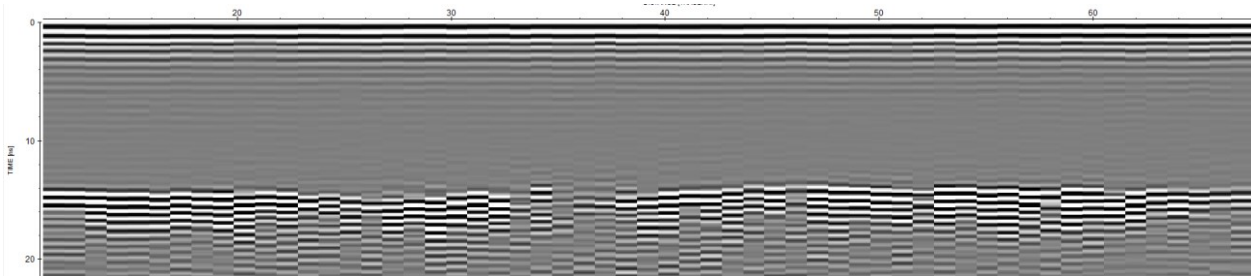

Figure S9. 6 Feb South Base radargram.

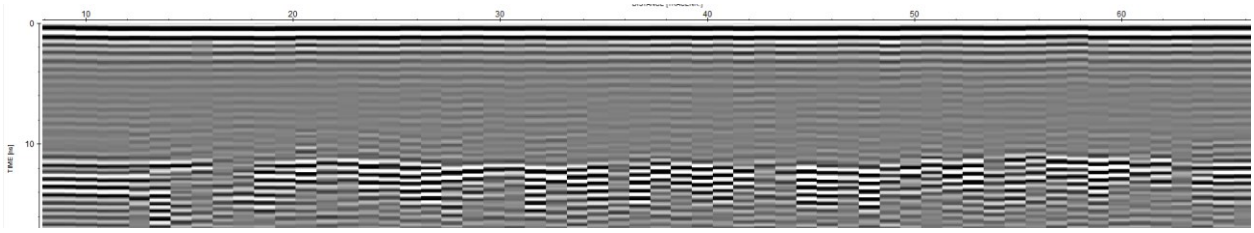

Figure S10. 6 Feb South Middle radargram.

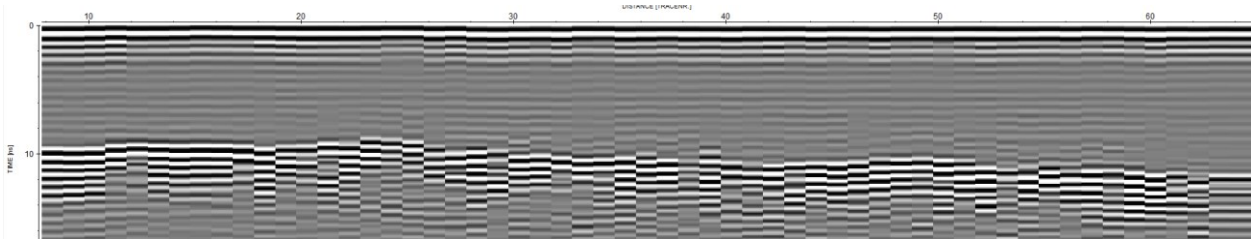

Figure S11. 6 Feb South Top radargram.

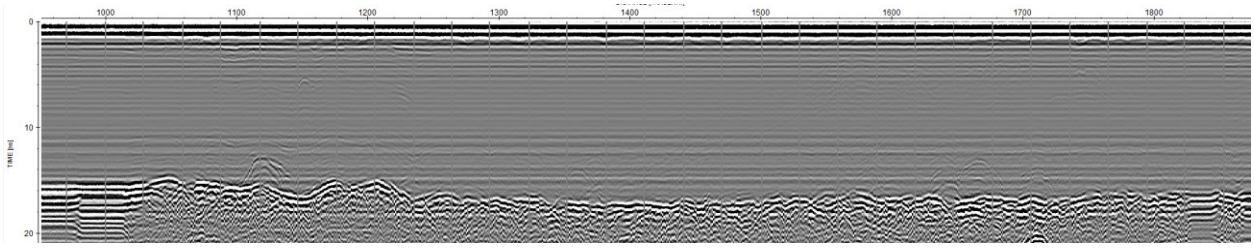

Figure S12. 25 Feb Flat aspect radargram.

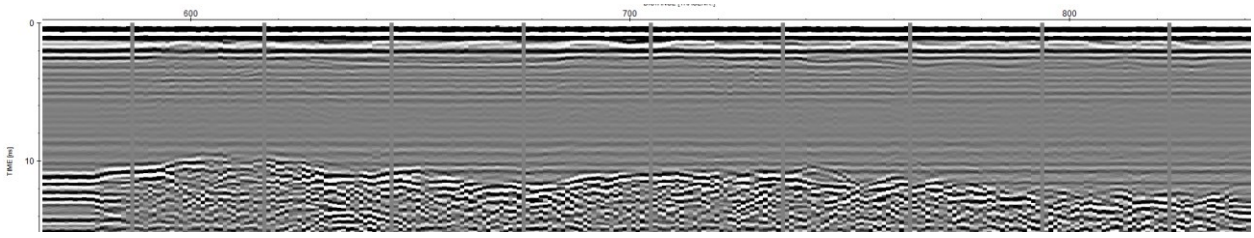

Figure S13. 25 Feb North Base radargram.

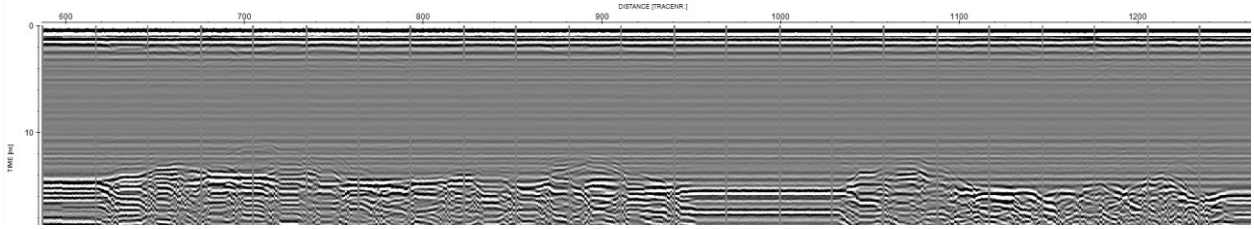

Figure S14. 25 Feb North Middle radargram.

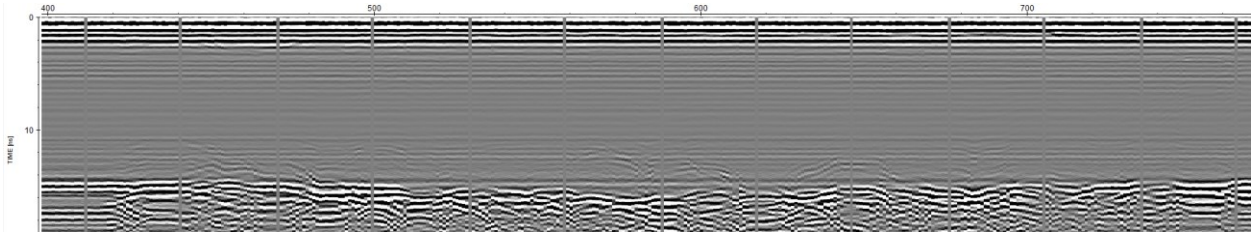

Figure S15. 25 Feb North Top radargram.

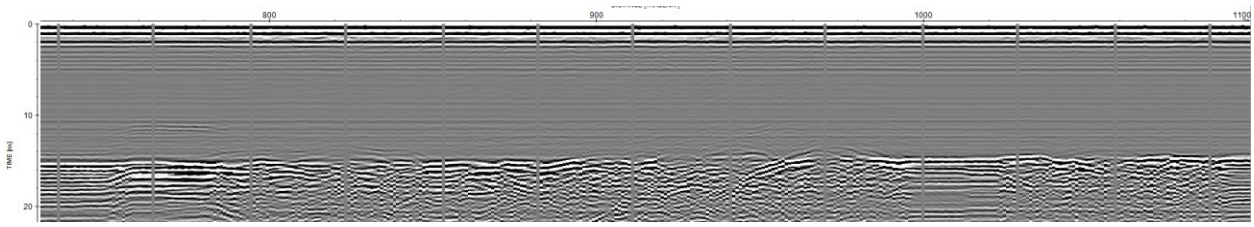

Figure S16. 25 Feb South Base radargram.

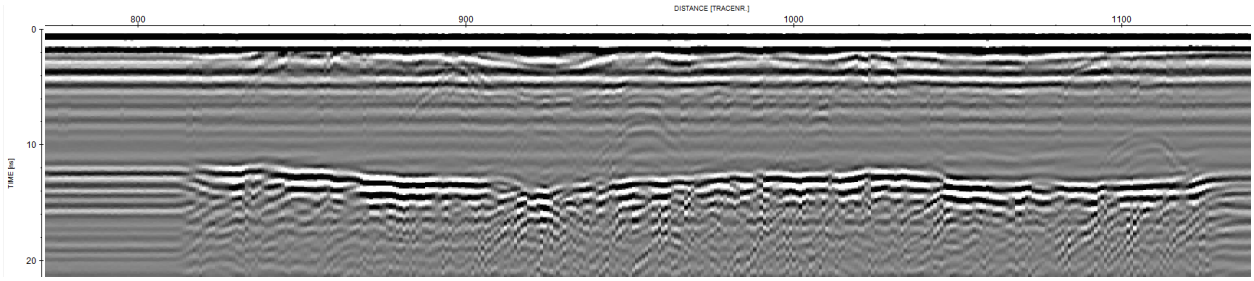

Figure S17. 25 Feb South Middle radargram.

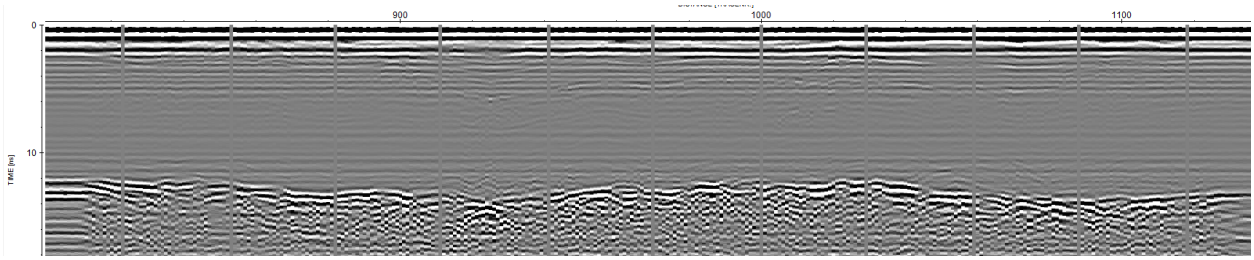

Figure S18. 25 Feb South Top radargram.

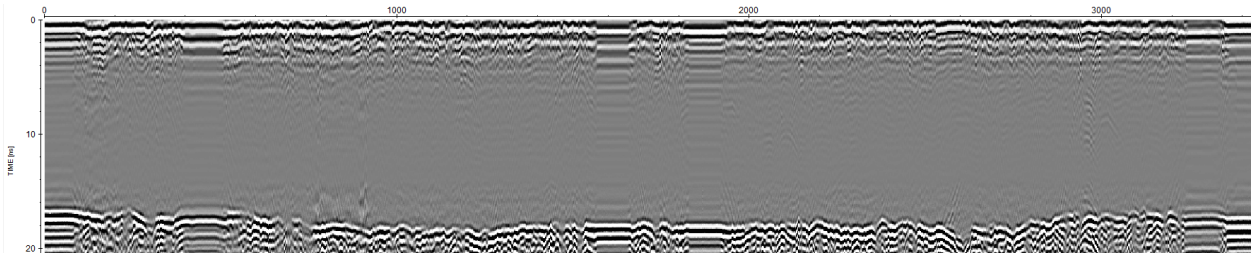

Figure S19. 1 Apr Flat aspect radargram.

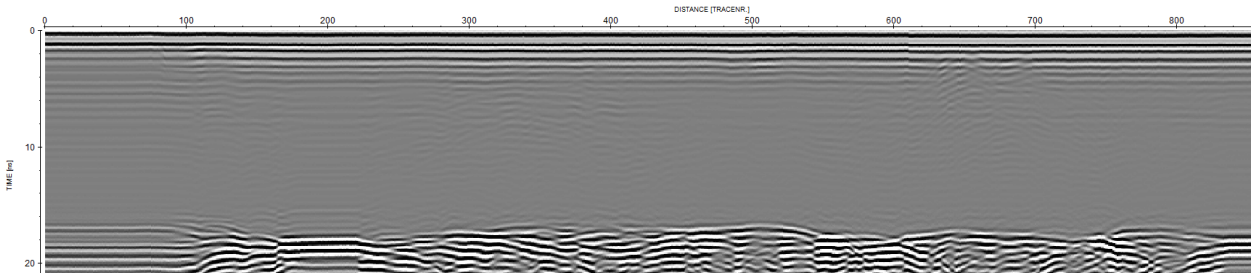

Figure S20. 1 Apr North Base radargram.

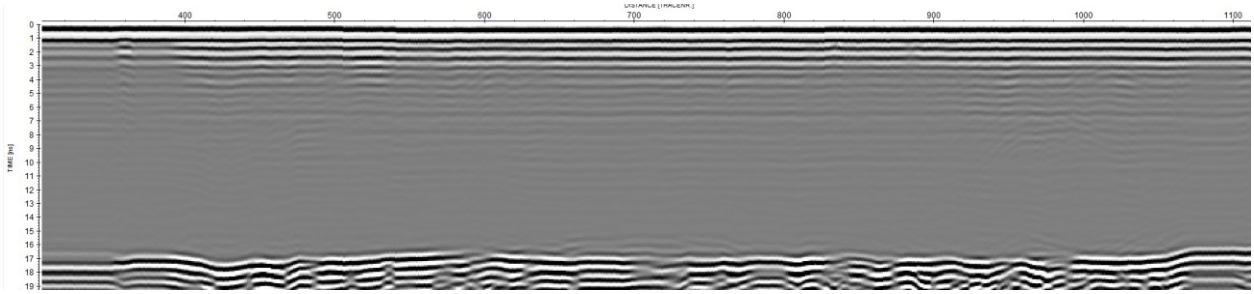

Figure S21. 1 Apr North Middle radargram.

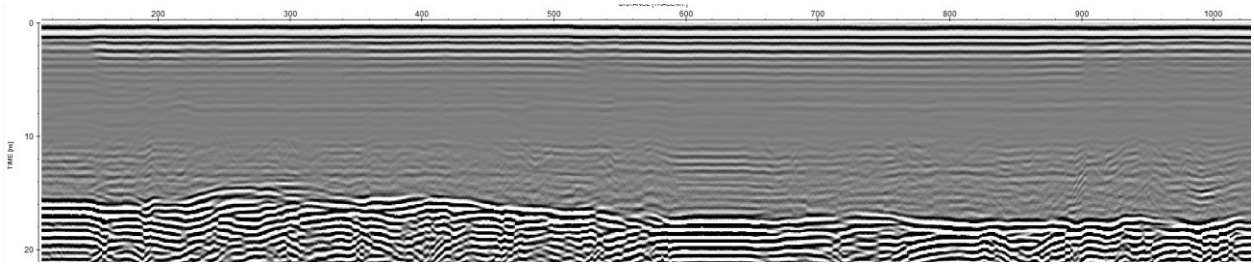

Figure S22. 1 Apr North Top radargram.

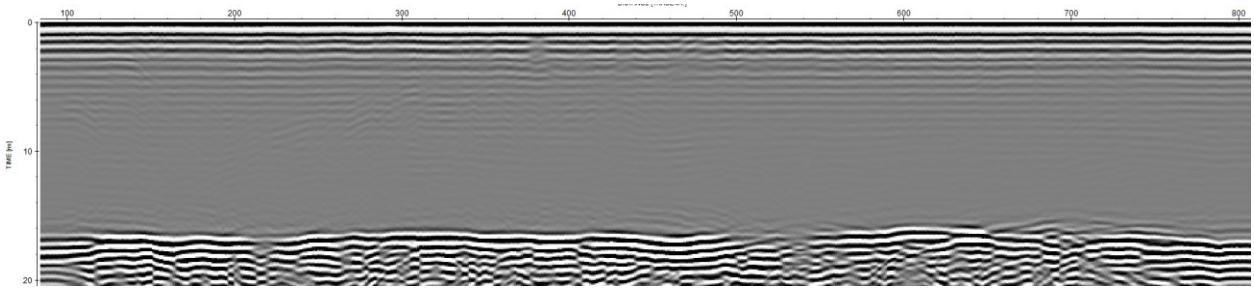

Figure S23. 1 Apr South Base radargram.

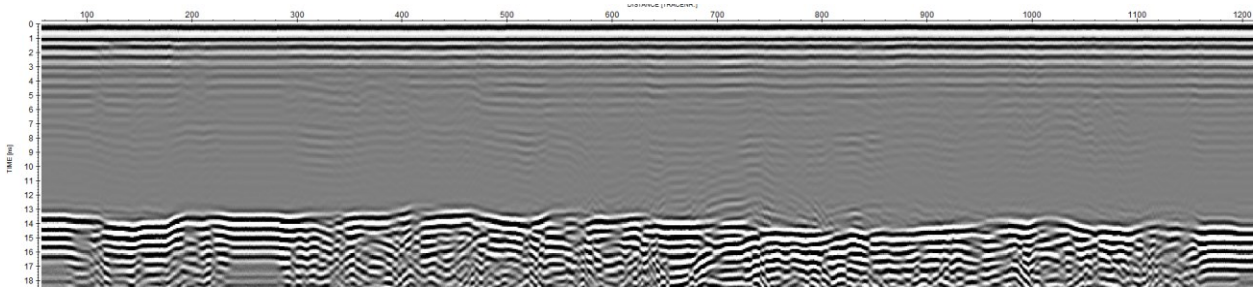

Figure S24. 1 Apr South Middle radargram.

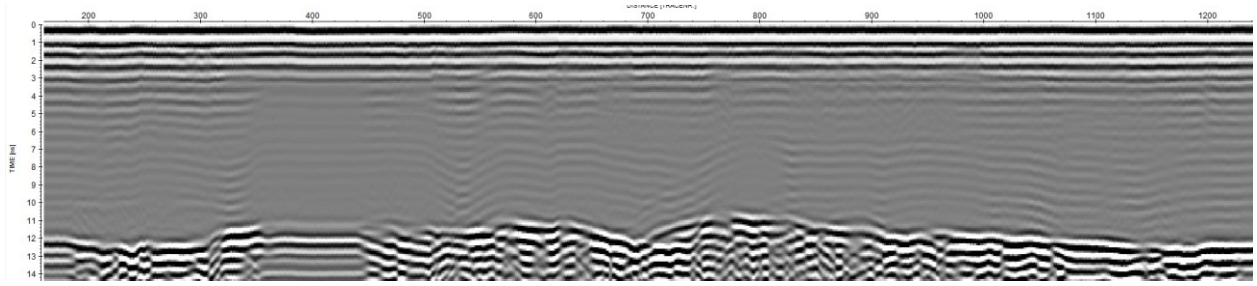

Figure S25. 1 Apr South Top radargram.

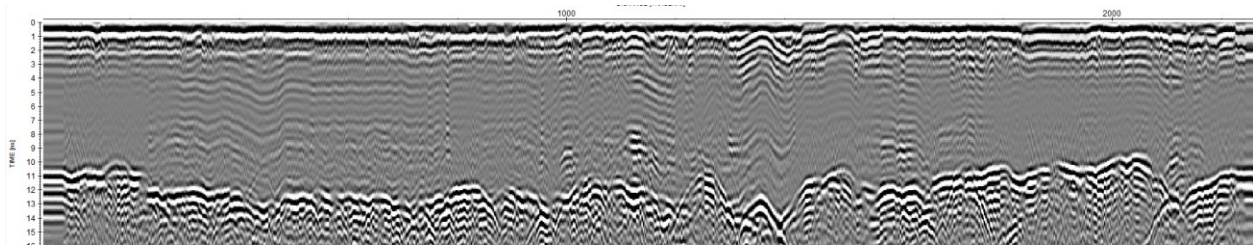

Figure S26. 1 May Flat aspect radargram.

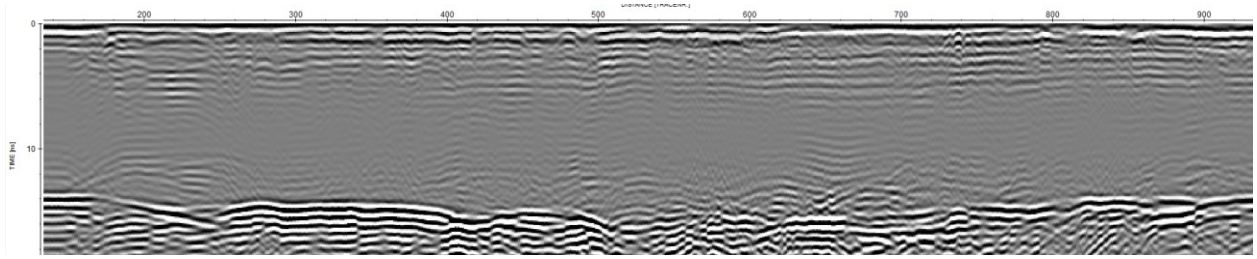

Figure S27. 1 May North Base radargram.

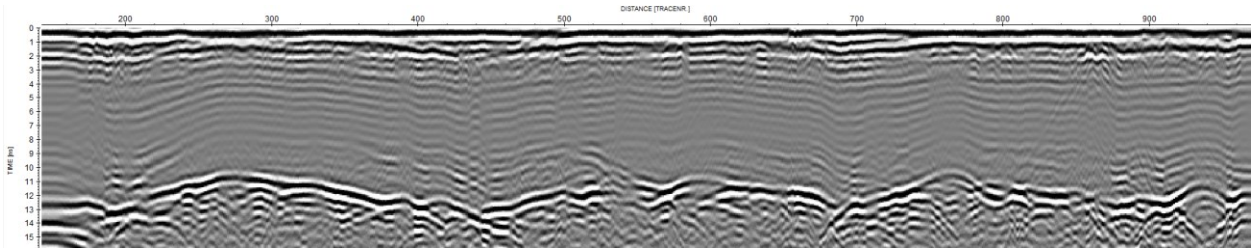

Figure S28. 1 May North Middle radargram.

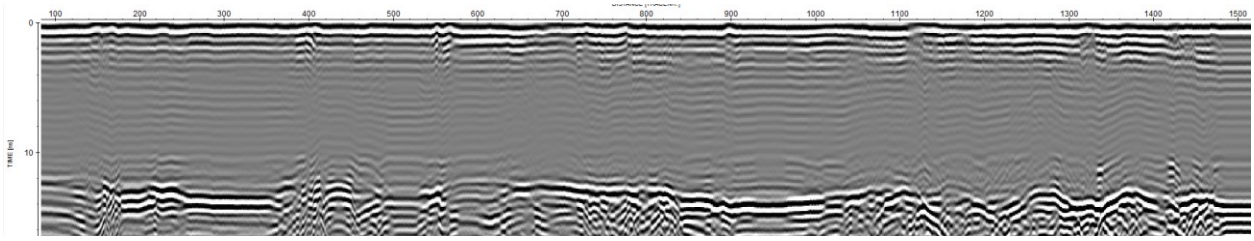

Figure S29. 1 May North Top radargram.

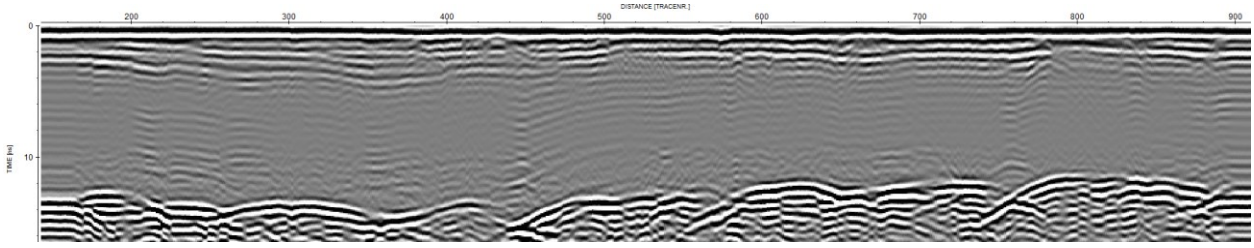

Figure S30. 1 May South Base radargram.

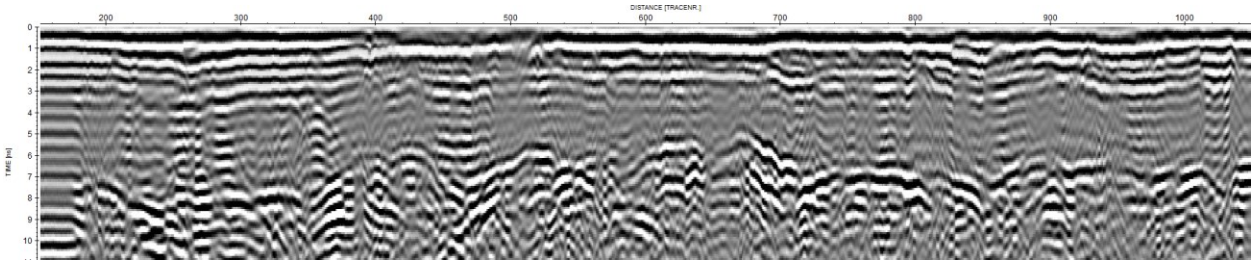

Figure S31. 1 May South Middle radargram.

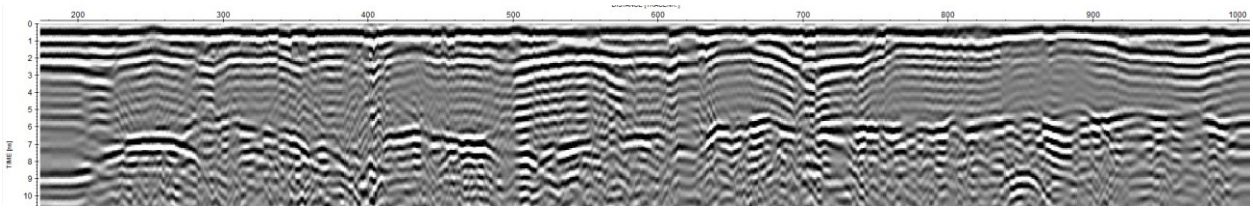

Figure S32. 1 May South Top radargram.